

# ANALYSIS OF SPECTRAL REMOTE SENSING DATA FOR GEOLOGICAL MAPPING OF RARE EARTH ELEMENTS (CASE STUDY OF THE KOLA PENINSULA)

A. A. Kamaev<sup>1,2</sup> 

<sup>1</sup>Geophysical Center of the Russian Academy of Sciences, Moscow, Russia

<sup>2</sup>National University of Science and Technology MISIS, Moscow, Russia

\* **Correspondence to:** Artem Kamaev, a.kamaev@gcras.ru

Rare earth elements (REEs) are strategically important components of modern industry; however, their exploration and extraction are complicated by the limited number of deposits and the difficulty of detection. This paper examines current approaches to the use of hyperspectral and multispectral remote sensing data for REE mapping, including data processing methods, analysis of key spectral characteristics, and examples of successful applications. Special attention is given to adaptive cosine estimator. Using the Khibiny Massif as a case study, the significance of combining direct spectral indicators of REE-bearing minerals with indirect indicators related to metasomatic zoning is demonstrated. The results confirm the effectiveness of the integrated application of spectral methods and thematic classification for detecting REEs in the complex geological conditions of the Arctic zone.

**Keywords:** Rare earth elements, hyperspectral remote sensing, remote exploration methods, spectral analysis, mineral deposit mapping.

**Citation:** Kamaev A. A. (2025), Analysis of Spectral Remote Sensing Data for Geological Mapping of Rare Earth Elements (Case Study of the Kola Peninsula), *Russian Journal of Earth Sciences*, 25, ES6008, EDN: KBFOBZ, <https://doi.org/10.2205/2025ES001077>

## Introduction

Rare earth elements (REEs) represent a group of 17 metals, including the lanthanides, scandium, and yttrium, which possess unique physicochemical properties highly demanded in high-technology industries [Balaram, 2019]. Despite their relatively high abundance in the Earth's crust, economically significant REE deposits are rare, making them strategically important resources [Goodenough et al., 2017]. Traditional exploration methods, such as geochemical analysis and geophysical surveys, require considerable time and financial expenditures, which stimulates the search for more efficient approaches, including the use of remote sensing data analysis.

Spectral methods, based on the analysis of reflected electromagnetic radiation, allow the identification of REEs by their characteristic narrow absorption bands in the visible and near-infrared ranges (VNIR, 400–1000 nm) [Turner et al., 2014]. For example, monazite, an important concentrator mineral of light rare earth elements, is characterized by pronounced absorption bands associated with Nd<sup>3+</sup> and Pr<sup>3+</sup> ions in the visible and near-infrared ranges. The most stable and diagnostically significant bands are recorded around ~580 nm, ~740 nm, ~800–820 nm, and ~870 nm, while less intense bands are also observed in the near-infrared range (1.3–1.6 μm) [Boesche et al., 2016, 2015] (Figure 1).

Hyperspectral remote sensing data can be obtained from satellite systems such as Resurs-P, EnMAP, Hyperion, PRISMA, and others, as well as from airborne surveys using

## RESEARCH ARTICLE

Received: 2025-09-10

Accepted: 2025-11-10

Published: 2025-12-10



**Copyright:** © 2025. The Author.  
This article is an open access article distributed under the terms and conditions of the Creative Commons Attribution (CC BY) license (<https://creativecommons.org/licenses/by/4.0>).

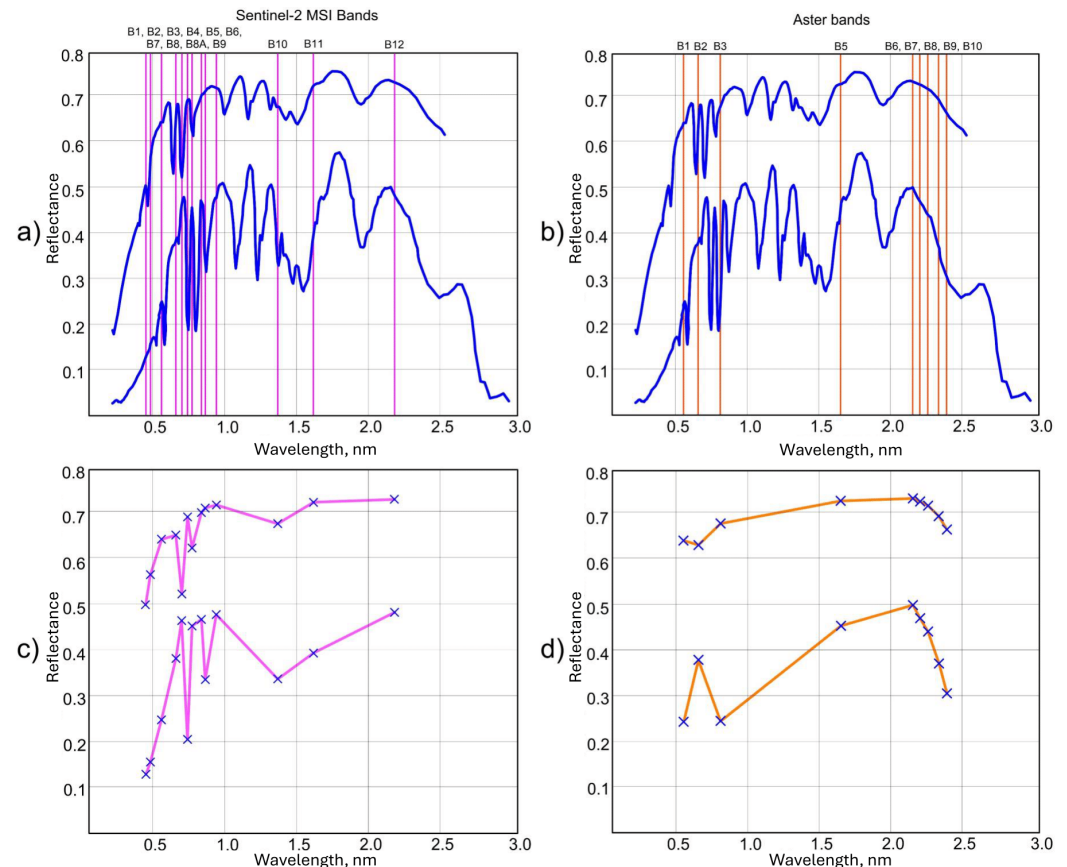


**Figure 1.** a, b – laboratory spectra of monazite [Kokaly *et al.*, 2017] and the positions of Sentinel-2 MSI and ASTER channels; vertical lines indicate the centers of the channel ranges; c, d – monazite spectra resampled to the spectral resolution of Sentinel-2 MSI and ASTER.

specialized hyperspectral imaging instruments (HySpex, Resonon, Cubert, etc.). The resulting data provides high spectral resolution necessary for detecting the narrow absorption bands of REEs [Kokaly *et al.*, 2017]. For example, in the study [Mars, 2018], Richardson-Lucy deconvolution was applied to airborne HySpex data to enhance spectral reflection signals of Nd in Norwegian carbonatites, enabling the creation of high-quality REE distribution maps even under suboptimal lighting conditions. Another example is the work [Asadzadeh *et al.*, 2024a], where EnMAP data were successfully used to map Nd at the Mountain Pass deposit (California) with a spatial accuracy of up to 30 m.

However, the successful detection of REEs depends on multiple factors, including the concentration levels of the elements, the presence of interfering minerals (e.g., iron oxides), vegetation cover, and the quality of atmospheric correction [Mars, 2018]. For instance, even 1% of iron oxides can suppress REE signals, particularly in the ~580 nm region [Herrmann, 2015].

Thus, the aim of this paper is to examine modern methods, technologies, and hyperspectral remote sensing data for geological mapping and prediction of REE deposits, as well as their practical application in the Arctic zone of the Russian Federation, specifically using the Khibiny Massif in the Murmansk region as a case study.

### Study Area

The Khibiny Massif is located in the central part of the Kola Peninsula, within the Fennoscandian Shield, and belongs to the Kola Alkaline Province (Figure 2). It is a large multiphase ring-shaped alkaline intrusion (with an area of about 1300 km<sup>2</sup>), composed of a series of nepheline syenites and foidolites (khibinites, rischorrites, urtites, ijolites, etc.) with late carbonatites. The sequence of magmatic phases is clearly expressed concentrically

from the margins to the center. Within the massif, giant world-class apatite-nepheline ore fields are localized, which have been industrially exploited since the 1930s [Kalashnikov *et al.*, 2016; Kogarko, 2018].

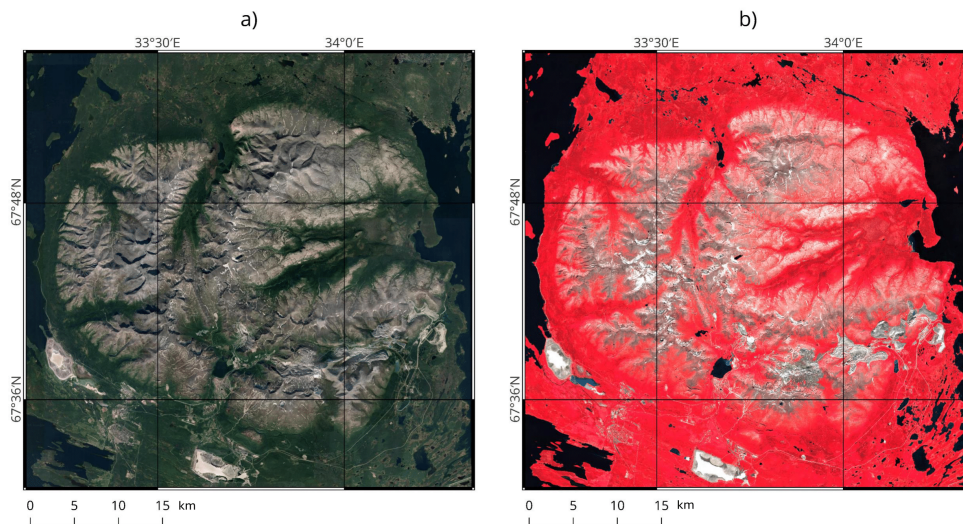


**Figure 2.** Satellite images of the Khibiny Massif. a – natural color composite (RED-GREEN-BLUE); b – infrared channel composite (NIR-RED-GREEN).

Geochronologically, the formation of the ore-magmatic system of the Khibiny (and the neighboring Lovozero) Massif dates to the Late Devonian-Early Carboniferous (about 380–370 Ma), as confirmed by U–Pb SHRIMP dating of titanite and consistent with data on the subalkaline rock series of the complex [Arzamastsev *et al.*, 2024; Rodionov *et al.*, 2018]. These results constrain the duration of the system’s activity to 15–20 million years and associate it with plume magmatism in eastern Fennoscandia.

The mineralogical and geochemical specificity of the massif is critical for remote sensing tasks related to REE mapping. The main REE concentrator in the Khibiny ores is fluorapatite from the apatite-nepheline bodies, enriched in light REEs (LREEs) and strontium. The typical total REE content in apatite reaches ~0.9 wt% REE<sub>2</sub>O<sub>3</sub> (average across several deposits), with a Ce/Yb ratio of ~680 and only a weakly expressed negative Eu anomaly [Kogarko, 2018; Kogarko, 2023]. Titanite, nepheline, aegirine, and titanomagnetite form complex (associated) ores and tailings, locally enriched in Ti and rare metals [Gerasimova *et al.*, 2018]. These features reflect prolonged fractional crystallization and convective stratification of the urtite-ijolite magmatic chamber, where fine-grained apatite accumulated in the upper parts of the chambers, and nepheline – in the lower parts (urtites) [Kogarko, 2018; Kogarko, 2023].

Structurally and tectonically, the massif is associated with the zone of Neoproterozoic-Paleozoic reactivations of eastern Fennoscandia; zones of fenitization and alkaline metasomatites developed around the large foidolite bodies. These halos, together with the levels of enrichment in apatite, loparite, and eudialyte in the regional province (Khibiny-Lovozero), record the conditions of early saturation of magmas with phosphorus and rare metals, and control the localization of ore bodies [Kogarko, 2023].

### Material and Methods

Visual analysis of spectral curves involves the direct comparison of recorded reflectance spectra with reference libraries (USGS Spectral Library, ECOSTRESS, SPECCHIO) to identify characteristic absorption bands. For REE-bearing minerals such as monazite, bastnäsite, xenotime, and eudialyte, the key features are narrow bands caused by electronic transitions of Nd<sup>3+</sup>, Pr<sup>3+</sup>, Sm<sup>3+</sup>, Dy<sup>3+</sup> ions and others. The most stable bands are observed in the ranges

of 0.58–0.60  $\mu\text{m}$ ,  $\sim 0.74 \mu\text{m}$ , 0.80–0.82  $\mu\text{m}$ ,  $\sim 0.87 \mu\text{m}$ , as well as weaker absorptions in the near-infrared (1.3–1.6  $\mu\text{m}$ ).

For the quantitative assessment of band depth, the continuum removal (CR) method is applied. For a spectrum  $R(\lambda)$ , the continuum line  $C(\lambda)$  is constructed as a linear or convex hull connecting points outside the absorption band. The normalized spectrum is then calculated as:

$$R_{CR}(\lambda) = \frac{R(\lambda)}{C(\lambda)}.$$

Band depth:

$$BD = 1 - \min(R_{CR}(\lambda)).$$

Band area:

$$BA = \sum_{\lambda_1}^{\lambda_2} [1 - R_{CR}(\lambda)] \Delta\lambda.$$

Threshold values of  $BD$  and  $BA$  are determined based on laboratory spectra of reference minerals. Narrow REE bands may be obscured by atmospheric artifacts or low spectral resolution, particularly in Sentinel-2 data, where the channel widths exceed the width of  $\text{Nd}^{3+}$  absorption bands. This necessitates verification with hyperspectral measurements.

For target detection, the Adaptive Cosine Estimator (ACE) method is used, which is widely applied in hyperspectral and multispectral analysis [Karimzadeh and Tangestani, 2022]. This is a spectral detection technique designed to identify pixels whose spectral signature corresponds to a given reference reflectance vector. The method belongs to the class of detectors based on matched filtering and accounts for both the direction and amplitude of the spectral vector, normalized to the statistical characteristics of the background environment.

The mathematical formulation of the problem consists in evaluating the similarity between the spectrum of the investigated pixel  $x$  and the target spectrum  $s$ , taking into account the covariance matrix of the background  $K$ , which describes the inter-channel relationships and suppresses the influence of correlated noise. The normalized ACE metric is calculated as follows:

$$ACE(x) = \frac{(s^T K^{-1} x)^2}{(s^T K^{-1} s)(x^T K^{-1} x)},$$

where  $s^T$  is the transposed target spectrum vector,  $K^{-1}$  is the inverse covariance matrix of the background signal, and  $x$  is the spectral value vector of the pixel.

ACE values range from 0 to 1, where 0 corresponds to no similarity and 1 corresponds to a complete match of spectra, taking into account background statistics.

In practical applications, the ACE method is used for the detection and mapping of minerals, vegetation communities, infrastructure objects, and other target classes, provided that their reference spectrum is known or measured. In the case of multispectral data, such as Sentinel-2, ACE calculation requires preliminary normalization of reflectance values and adaptation of the reference spectrum to the sensor's spectral discretization.

The key advantages of ACE include its scale invariance – meaning that the evaluation is independent of the absolute illumination level – as well as its ability to suppress background correlations through the use of the inverse covariance matrix, thereby reducing the probability of false positives under spectrally heterogeneous background conditions.

## Results

Modern approaches to rare earth element (REE) studies are based on the integrated analysis of hyperspectral remote sensing data, which provide detailed information on the composition of the Earth's surface. The key advantage of hyperspectral systems lies in their ability to record reflected radiation across hundreds of narrow spectral channels (typically 5–10 nm) spanning the visible to short-wave infrared range (400–2500 nm) [Asadzadeh and



*de Souza Filho, 2016*]. This level of detail enables the detection of the narrow absorption bands characteristic of REEs.

The significance of the Khibiny area for remote REE mapping is determined by two groups of indicators: direct spectral features of REE-bearing minerals and indirect signs related to host rocks and metasomatic zoning. In the VNIR-SWIR range (0.4–2.5  $\mu\text{m}$ ), REEs produce narrow f–f absorption bands ( $\text{Nd}^{3+}$ ,  $\text{Pr}^{3+}$ ,  $\text{Sm}^{3+}$ , etc.) in minerals such as monazite, xenotime, and bastnäsite. Although apatite exhibits lower spectral diagnostic capability, the combination of weak REE bands with phosphate, carbonate, and silicate features, as well as luminescent properties (Mn centers,  $\text{Eu}^{2+}$ ), enhances interpretive selectivity under conditions of high signal-to-noise ratio (SNR) and hyperspectral resolution [*Koerting et al., 2021; Van der Meer et al., 2012*]. Recent studies have demonstrated successful identification of REE minerals in the VNIR-SWIR range using satellite hyperspectral imaging (e.g., EnMAP) and specialized spectral libraries [*Asadzadeh et al., 2024b; Van der Meer et al., 2012*]. For provinces with alkaline and carbonatitic associations, diagnostic potential has been shown for combinations of REE fluorocarbonate bands with those of background carbonates/fenites [*Rowan and Mars, 2003; Van der Meer et al., 2012*].

From a practical standpoint, this implies that for remote sensing applications in the Khibiny area it is advisable to: focus on hyperspectral sensors with  $\leq 10$  nm sampling in the VNIR and high sensitivity in the SWIR; employ spectral library references for REE minerals and apatite, cross-checking them with laboratory spectra of thin sections and loose samples; and map fenitization halos as indicators of alkaline magmatism and secondary processes by combining spectral indices of carbonates, phosphates, and Fe-Mg silicates with subpixel decomposition and target classification methods [*Asadzadeh et al., 2024b; Van der Meer et al., 2012*].

To identify potential REE-enriched areas within the Khibiny Massif, the ACE metric was calculated. The resulting values were transformed into discrete classes, each corresponding to a specific ACE interval and represented by a designated color scale, which provides clarity in interpreting the results. The applied six-class scale divided the ACE range from 0 to 1 into the following intervals: 0.000–0.166 – very low similarity (dark blue), 0.167–0.333 – low (light blue), 0.334–0.499 – moderately low (lime green), 0.500–0.666 – moderate (yellow), 0.667–0.833 – moderately high (orange), and 0.834–1.000 – very high, nearly complete match (bright red). Based on the calculations, an ACE distribution map was compiled highlighting areas with potentially high REE concentrations (*Figure 3*).

Correct interpretation of ACE results requires consideration not only of the numerical values of the metric but also of the geomorphological context of the area. High ACE values may occur not only over target mineralized zones but also on anthropogenic objects (roads, dumps, construction sites) (lower part of *Figure 3*), where the spectral signature may coincidentally resemble the reference spectrum. Therefore, final ACE maps should be analyzed in conjunction with additional masks (vegetation, built-up areas, water bodies, relief) and expert interpretation, which makes it possible to eliminate false-positive detections and highlight only those anomalies that are reasonably associated with geological features.

## Conclusions

The analysis of remote sensing data represents a promising approach for the identification and mapping of rare earth element (REE) deposits, owing to its ability to capture narrow absorption bands characteristic of  $\text{Nd}^{3+}$ ,  $\text{Pr}^{3+}$ ,  $\text{Sm}^{3+}$ , and other REE ions in concentrator minerals (e.g., monazite). Studies conducted on the Khibiny Massif demonstrated that the application of the Adaptive Cosine Estimator not only enhances interpretive selectivity but also delineates spectrally similar zones with a high probability of containing target minerals. Mapping fenitization and alkaline metasomatic halos complements the spectral indicators and improves the reliability of predicting ore body localization. Thus, the integration of spectral methods with mineralogical and geochemical data, reference spectra, and structural-tectonic analysis provides a foundation for a more accurate assessment of

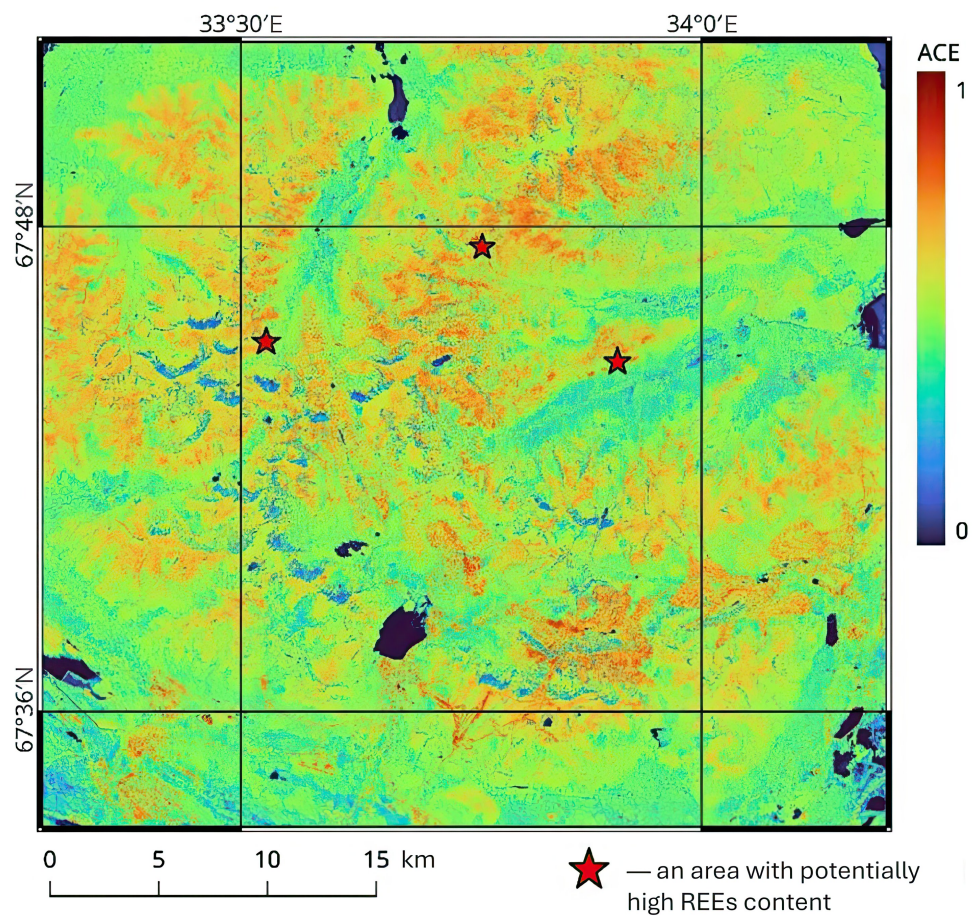


**Figure 3.** Map of ACE values across the Khibiny Massif highlighting potential rare earth element (REE) zones.

the REE potential of territories, and the approaches obtained can be scaled for application in other regions with similar geological conditions.

**Acknowledgments.** This work was conducted in the framework of budgetary funding of the Geophysical Center of RAS, adopted by the Ministry of Science and Higher Education of the Russian Federation. This work employed facilities and data provided by the Shared Research Facility “Analytical Geomagnetic Data Center” of the Geophysical Center of RAS (<http://ckp.gcras.ru/>). The author gratefully acknowledges the reviewers for their valuable comments and the journal editor for the careful revision and improvement of the manuscript.

## References

- Arzamastsev A. A., Ivanova A. A., Salnikova E. B., et al. Age and Origin of the Subalkaline Magmatic Series of the Khibiny-Lovozero Complex // *Petrology*. — 2024. — Vol. 32, no. 3. — P. 337–358. — <https://doi.org/10.1134/s0869591124700024>.
- Asadzadeh S. and de Souza Filho C. R. A review on spectral processing methods for geological remote sensing // *International Journal of Applied Earth Observation and Geoinformation*. — 2016. — Vol. 47. — P. 69–90. — <https://doi.org/10.1016/j.jag.2015.12.004>.
- Asadzadeh S., Koellner N. and Chabrilat S. Detecting rare earth elements using EnMAP hyperspectral satellite data: a case study from Mountain Pass, California // *Scientific Reports*. — 2024a. — Vol. 14, no. 1. — <https://doi.org/10.1038/s41598-024-71395-2>.

- Asadzadeh S., Koellner N. and Chabrilat S. Detecting rare earth elements using EnMAP hyperspectral satellite data: a case study from Mountain Pass, California // *Scientific Reports*. — 2024b. — Vol. 14, no. 1. — P. 20766. — <https://doi.org/10.1038/s41598-024-71395-2>.
- Balaram V. Rare earth elements: A review of applications, occurrence, exploration, analysis, recycling, and environmental impact // *Geoscience Frontiers*. — 2019. — Vol. 10, no. 4. — P. 1285–1303. — <https://doi.org/10.1016/j.gsf.2018.12.005>.
- Boesche N. K., Mielke C., Segl K., et al. Hyperspectral Rare Earth Element Mapping of Three Outcrops at the Fen Complex, Norway // *Rare Earths Industry: Technological, Economic, and Environmental Implications*. — 2016. — P. 235–265. — <https://doi.org/10.1016/b978-0-12-802328-0.00016-4>.
- Boesche N. K., Rogass C., Lubitz C., et al. Hyperspectral REE (Rare Earth Element) Mapping of Outcrops-Applications for Neodymium Detection // *Remote Sensing*. — 2015. — Vol. 7, no. 5. — P. 5160–5186. — <https://doi.org/10.3390/rs70505160>.
- Gerasimova L. G., Nikolaev A. I., Maslova M. V., et al. Titanite Ores of the Khibiny Apatite-Nepheline-Deposits: Selective Mining, Processing and Application for Titanosilicate Synthesis // *Minerals*. — 2018. — Vol. 8, no. 10. — P. 446. — <https://doi.org/10.3390/min8100446>.
- Goodenough K. M., Wall F. and Merriman D. The Rare Earth Elements: Demand, Global Resources, and Challenges for Resourcing Future Generations // *Natural Resources Research*. — 2017. — Vol. 27, no. 2. — P. 201–216. — <https://doi.org/10.1007/s11053-017-9336-5>.
- Herrmann S. Capacity of Imaging Spectroscopy for the Characterization of REO, REE Bearing Minerals & Primary REE-Deposits, Master Thesis (Scientific Technical Report; 19/08). — Potsdam, Germany : University of Potsdam, 2015. — 210 p. — <https://doi.org/10.2312/GFZ.b103-19089>.
- Kalashnikov A. O., Konopleva N. G., Pakhomovsky Ya. A., et al. Rare Earth Deposits of the Murmansk Region, Russia-A Review // *Economic Geology*. — 2016. — Vol. 111, no. 7. — P. 1529–1559. — <https://doi.org/10.2113/econgeo.111.7.1529>.
- Karimzadeh S. and Tangestani M. H. Potential of Sentinel-2 MSI data in targeting rare earth element (Nd3+) bearing minerals in Esfordi phosphate deposit, Iran // *The Egyptian Journal of Remote Sensing and Space Sciences*. — 2022. — Vol. 25, no. 3. — P. 697–710. — <https://doi.org/10.1016/j.ejrs.2022.04.001>.
- Koerting F., Koellner N., Kuras A., et al. A solar optical hyperspectral library of rare-earth-bearing minerals, rare-earth oxide powders, copper-bearing minerals and Apliki mine surface samples // *Earth System Science Data*. — 2021. — Vol. 13, no. 3. — P. 923–942. — <https://doi.org/10.5194/essd-13-923-2021>.
- Kogarko L. Chemical Composition and Petrogenetic Implications of Apatite in the Khibiny Apatite-Nepheline Deposits (Kola Peninsula) // *Minerals*. — 2018. — Vol. 8, no. 11. — P. 532. — <https://doi.org/10.3390/min8110532>.
- Kogarko L. N. Rare Earth Element Resource Potential of Super-Large Deposits in Eastern Fennoscandia // *Doklady Earth Sciences*. — 2023. — Vol. 513, no. 2. — P. 1296–1300. — <https://doi.org/10.1134/s1028334x23602067>.
- Kokaly R. F., Clark R. N., Swayze G. A., et al. USGS Spectral Library Version 7. — US Geological Survey, 2017. — 61 p. — <https://doi.org/10.3133/ds1035>.
- Mars J. C. Mineral and Lithologic Mapping Capability of WorldView 3 Data at Mountain Pass, California, Using True- and False-Color Composite Images, Band Ratios, and Logical Operator Algorithms // *Economic Geology*. — 2018. — Vol. 113, no. 7. — P. 1587–1601. — <https://doi.org/10.5382/econgeo.2018.4604>.
- Rodionov N. V., Lepekhina E. N., Antonov A. V., et al. U-Pb SHRIMP-II ages of titanite and timing constraints on apatite-nepheline mineralization in the Khibiny and Lovozero alkaline massifs (Kola Peninsula) // *Russian Geology and Geophysics*. — 2018. — Vol. 59, no. 8. — P. 962–974. — <https://doi.org/10.1016/j.rgg.2018.07.016>.
- Rowan L. C. and Mars J. C. Lithologic mapping in the Mountain Pass, California area using Advanced Spaceborne Thermal Emission and Reflection Radiometer (ASTER) data // *Remote Sensing of Environment*. — 2003. — Vol. 84, no. 3. — P. 350–366. — [https://doi.org/10.1016/S0034-4257\(02\)00127-X](https://doi.org/10.1016/S0034-4257(02)00127-X).
- Turner D. J., Rivard B. and Groat L. A. Visible and short-wave infrared reflectance spectroscopy of REE fluorocarbonates // *American Mineralogist*. — 2014. — Vol. 99, no. 7. — P. 1335–1346. — <https://doi.org/10.2138/am.2014.4674>.
- Van der Meer F. D., van der Werff H. M. A., van Ruitenbeek F. J. A., et al. Multi- and hyperspectral geologic remote sensing: A review // *International Journal of Applied Earth Observation and Geoinformation*. — 2012. — Vol. 14, no. 1. — P. 112–128. — <https://doi.org/10.1016/j.jag.2011.08.002>.